Enhanced production of ^{24}Na by wide-angle secondaries produced in the interaction of relativistic carbon ions with copper

R. Brandt, G. Dersch, E. M. Friedlander,* G. Haase, and M. Heck
Kernchemie, Philipps-University, Marburg, Germany

V. S. Butsev, M. I. Krivopustov, and B. A. Kulakov
Joint Institute for Nuclear Research, Dubna, Russia

E.-J. Langrock and F. Pille
Fachbereich Naturwissenschaft, Technische Hochschule, Leipzig, Germany

H. H. Cui
Insitute for High Energy Physics, Beijing, People's Republic of China

E. Ganssauge
Fachbereich Physik, Philipps-University, Marburg, Germany
(Received 3 September 1991)

Radiochemical activation techniques were used to study the behavior of projectile fragments formed in the interaction of 44 GeV ^{12}C ions within thick Cu targets. After a short review of the results obtained hitherto with this Cu-target technique, the interaction of 44 GeV ^{12}C with several copper target configurations yielding the deep spallation product ^{24}Na is described. Energetic fragments which are emitted into the laboratory angles $10° \leq \theta \leq 45°$ appear to produce more ^{24}Na (up to nearly one order of magnitude) than calculated with a phenomenological model and an intranuclear cascade model. This enhanced production of ^{24}Na by wide-angle secondaries is only observed for 44 GeV ^{12}C on copper, but not for 25 GeV ^{12}C on copper. Some normalization experiments with 4 GeV ^{4}He and 2.6 GeV p are described.

PACS number(s): 25.75.+r

I. INTRODUCTION

The experiments described in this paper are intended to extend to a much wider range of energies per nucleon a previous experiment [1–15] introducing a *sui generis* technique of "calorimetry" in the investigation of interaction properties of projectile fragments (PF) from relativistic heavy-ion collisions. The idea of the experiment as well as the peculiar target/detector setups (in several increasingly sophisticated geometries) were initially motivated by the ongoing debate on a possible anomalously shortened mean free path (abbreviated hereafter as SMFP) for nuclear interactions of such projectile fragments. Although, at the present stage of our investigation, our experimental results have not provided a clear-cut evidence neither for nor against such an effect, they *have* provided evidence for a very high partial cross section of ^{24}Na production by PF emitted at relatively wide angles to the incident heavy-ion beam. Whether or not this effect can be explained in terms of "conventional" relativistic heavy-ion physics was explored in Ref. [2] and will be discussed in connection with the new experimental evidence outlined in the present paper. However, in order to better explain the rationale underlying our technique, it seems useful to briefly review the experimental evidence which prompted this investigation.

Evidence for a SMFP was first observed in nuclear emulsions. Reference [16] gives the basic experimental facts together with their early history. Essentially, this effect consists of a considerably reduced mean free interaction path of heavy PF ($Z \geq 3$) within the first few centimeters after the interaction point where they were produced in the interaction of relativistic heavy ions with emulsion nuclei. This work stimulated a wide variety of investigations, with often conflicting results [16–28]. Of particular interest is the more recent supporting experimental evidence concerning this effect, obtained at the Joint Institute for Nuclear Research (JINR) at Dubna [29–31]. This field of investigation has been reviewed recently [32–37]. Some older references have been mentioned frequently [38–43]. However, one should remember some possible "prehistoric" evidence for SMFP, such as peculiar transition effects observed with very thick targets in cosmic rays by Roessle and Schopper [44] as early as 1954 and confirmed later by Varsimashvili [45], and possible evidence for SMFP of pions shortly after their emission from kaon decays reported by Alexander, Johnston, and O'Ceallaigh [46] in 1957. These SMFP effects have never been challenged experimentally, nor have they been understood from a theoretical point of view.

The interest in the SMFP effect was stressed by its hy-

*Permanent address: Lawrence Berkeley Laboratory, University of California, Berkeley, CA 94720.

pothetical connection with the possible appearance of "open color states" for quark-gluon matter, as formulated within certain quantum-chromodynamic models [34]. Due to such possible fundamental implications and especially to the wide-ranging controversy aroused by this subject, it seemed important to bring as many different techniques as possible to bear on this problem. Therefore, some time ago, several of us started an experimental program to investigate the interactions of relativistic heavy ions with relatively massive copper targets [1]. The radiochemcial activation technique has been used to search for the possible formation, interaction, and decay of anomalous projectile fragments.

To date, the most detailed investigation has been carried out at the BEVALAC of the Lawrence Berkeley Laboratory (LBL) in the interaction of 72 GeV ^{40}Ar and 36 GeV ^{40}Ar with copper. At the lower energy, we encountered no difficulties in trying to understand the experimental results in terms of conventional models and of the ensemble of available experimental facts. However, at the higher energy it was impossible to explain the large cross section of secondary fragments for producing ^{24}Na in copper within the framework of widely accepted theoretical models: in particular, one had severe difficulties in understanding the wide-angle emission $10° \leq \theta$ of energetic secondary fragments. Reference [2] gives a detailed account of the "conventional" arguments which failed to explain the effect.

Consequently, it was of interest to extend the investigation beyond the range of energies per nucleon covered by the BEVALAC, in the hope of observing some general new features of relativistic heavy-ion physics irrespective of whether SMFP's were involved or not.

We start this paper with a general survey of the corresponding experiments. Then a detailed experimental and theoretical account is given of our studies using the 44 GeV ^{12}C beam of the SYNCHROPHASOTRON at the JINR (Dubna). Calibration experiments with 4 GeV ^{4}He and 2.6 GeV p beams from SATURNE, Saclay, are also reported. In view of the negative result of a search for unexpected features in the reactions induced by the lower energy beam at the BEVALAC (36 GeV ^{40}Ar) one would *a fortiori* not expect any anomalous behavior of particles produced at the energies of the SATURNE Accelerator. None was found.

II. THE COPPER-DISK TECHNIQUE

A. Normalizing experiments with two Cu disks and 25 GeV ^{12}C ions

Our first experiment of this kind may serve as an intuitive illustration of our technical approach; it was carried out via a parasitic exposure to a 25 GeV ^{12}C beam of the BEVALAC, behind a thin target (< 500 mg/cm^2) [47]. It can be considered as an example of a low-energy experiment with relativistic carbon.

The principle of the experiment is illustrated in Fig. 1(a). Two 1 cm thick circular copper disks ($r = 4$ cm) were irradiated. Typically, $\approx 10^{12}$ ^{12}C ions passed through the Cu disks in a period of 2–4 h. The beam was

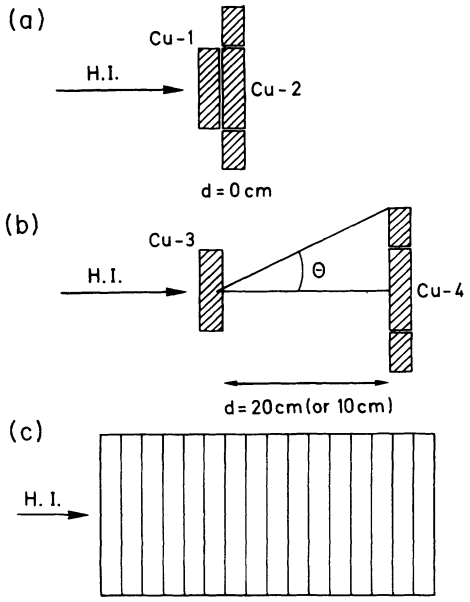

FIG. 1. Some typical experimental arrangements of Cu disks and rings. All Cu disks are 1 cm thick. (a),(b) Arrangement to study decay versus wide-angle effects as described in detail in [1,2]. (c) A very compact stack of 16 Cu disks ($\phi = 8$ cm) as a kind of calorimeter.

well focused (nominal diameter < 1 cm). Pairs of Cu disks were irradiated together in a "contact" configuration ($d = 0$ cm) and with a separation of 10 cm [Fig. 1(b)]. Both Cu disks serve as targets for the primary beam, as well as for secondaries interacting within the same disk in which they are produced. Our measure for the number of interactions induced by all these projectiles is the amount of radioactive residues of the target nuclei, detectable via their gamma activity. However, secondaries produced in the first disk (target) and interacting in the second disk (detector) will enhance radioactive nuclide production in the detector as compared to the target (assuming the same projectile flux). This enhancement could be especially strong if, among other things, such PF have an unexpectedly high interaction cross section, i.e, a "too short" mean free path. After the completion of the irradiation, short-lived activities were allowed to decay for approximately 12–24 h. Afterwards, the radionuclides present in the irradiated Cu disks were assayed by off-line gamma-ray spectrometry. Measurements were made with Ge(Li) detectors (resolution ≈ 1.8 keV for the 1332 keV line of ^{60}Co). The analysis of the gamma-ray spectra was based on standard radiochemical procedures [48]. Counting was carried out for approximately one week at Berkeley and then continued for several months at Marburg. For specific nuclides, we determined the ratio R_d of the activity in the detector (Cu-2, or Cu-4) to that in the target (Cu-1, or Cu-3) as a function of the separation d between target and detector. Because each such pair was irradiated with the same particle beam simultaneously and assayed later for its gamma activity in a fixed position with the same Ge(Li) gamma-ray detector, the activity ratio R_d for a specific

nuclide can be determined to a high degree of precision. All uncertainties due to particle fluxes, counting efficiencies, branching ratios in the decay scheme for a specified radioactive nuclide, etc., cancel out in R_d. Essentially, the only experimental uncertainty in R_d comes from counting statistics. The number of counts is typically $\geq 10^4$ with its corresponding precision, comparable only to that of large counter experiments or of high-statistic bubble chamber experiments.

We show in Fig. 2 the dependence of R_d on the product mass number A for two different separations ($d=0$ and 10 cm) for reactions induced by 25 GeV ^{12}C ions. This dependence is a reflection of the energy spectrum and angular distribution of the secondaries inducing reactions in the disks. The results show that when the two disks are in contact (R_0), the PF most likely to strike the detector lead to the formation (by target fragmentation) of products with $A \approx 55$ and substantial yields are seen for all products with $A > 40$. The products with $A < 30$ (^{7}Be, ^{22}Na, ^{24}Na, ^{28}Mg) are formed only in high-deposition energy target fragmentation events [49]. Such nuclides cannot be PF because those are much too energetic to stop in the copper disks. When the disks are moved 10 cm apart, the detector samples a different subset of the PF created in the target, i.e., the more strongly forward focused and thus higher energetic fragments. As a result, the PF most likely to reach the second disk now lead to the formation of products with $A \approx 45$ and the formation of heavier fragment is less likely. Not surprisingly, R_0 for these products is larger than R_{10}, reflecting production by low-energy, wide-angle secondaries. The fragments with $A < 30$ are produced with about the same yields regardless of disk separation because they are only produced by highly forward-focused, energetic PF. As we are interested mainly in reaction channels due practically only to relativistic high-energy particles (> 1 GeV),

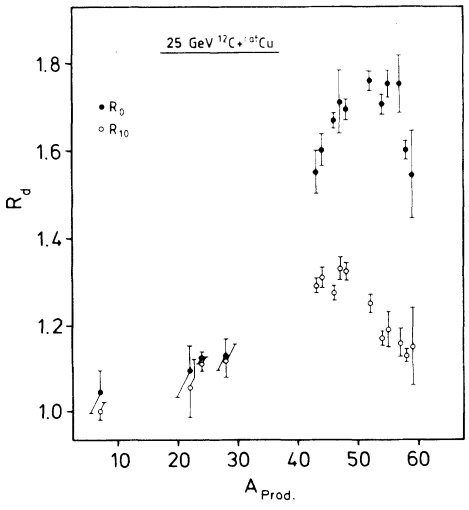

FIG. 2. R_0 and R_{10} as a function of the product mass A_{prod}. R_d is the ratio of the activity for one specific nuclide of the detector Cu disk to the target Cu disk, and d is the distance between both disks, as shown in Figs. 1(a) and 1(b). (This experiment was carried out at the BEVALAC, University of California, Berkeley.)

we concentrate on deep-spallation products ($A < 30$) since these nuclides are produced in copper only by high-energy particles. But, as Fig. 2 shows, only ^{24}Na can be measured with the necessary accuracy of $\approx(1-2)\%$. Therefore, we only concentrate our attention on the production of ^{24}Na from copper targets. Furthermore, the excitation function for the production of deep-spallation products is well known only for the production of ^{24}Na from Cu. Moreover, this nuclide has a half-life of ~ 15 h and a prominent and well-determined gamma line at $E_\gamma = 1.3685$ MeV, both very convenient for radiochemical experiments. In this experiment we observe for 25 GeV ^{12}C:

$$\frac{R_0(^{24}\text{Na})}{R_{10}(^{24}\text{Na})} = \frac{1.127\pm0.015}{1.108\pm0.017} = 1.017\pm0.021 , \quad (1)$$

$$R_0 - R_{10} = 0.019\pm0.023 . \quad (2)$$

All ^{24}Na-producing fragments are emitted within a laboratory angle $\theta < 20°$ in this experiment, as the $R_{10}(^{24}\text{Na})$ samples only fragments emitted into this angular forward cone. Our results reveal no unusual or anomalous properties of secondaries; all relativistic particles, primaries and secondaries, which produce ^{24}Na in the R_0 configuration seem to do nearly exactly the same in the R_{10} configuration.

To visualize this, one should consider the separate effects of three kinds of particles producing ^{24}Na: (a) beam projectiles (primaries) producing Q_P ^{24}Na atoms; (b) their secondaries (and the cascade products thereof) interacting in the same disk in which primaries interacted, producing Q_S ^{24}Na atoms; and (c) secondaries from the target interacting in the detector and producing there $Q_{S'} \approx 2Q_S$ atoms. It can be shown from Ref. [2], that, to a reasonable approximation, the ratio R_d is given by

$$R_d \approx \exp\left[-\frac{x}{\lambda_P}\right] + \frac{2(1-f_d)}{1+Q_P/Q_S} . \quad (3)$$

The first term on the right-hand side is the attenuation factor where x is the disk thickness (1 cm) and λ_P is the mean free path for inelastic collisions of the primaries. The factor f_d is the fraction of secondaries of type (c), above, which fail to reach the detector at distance d for one of the two reasons: (a) conversion of anomalous particles to normal particles; and/or (b) emission of energetic fragments into wide laboratory angles with $\theta > 20°$. As we observe $R_0 \approx R_{10}$ [Eq. (2)] we must conclude that $f_d \ll 1$. Consequently, we neither observe to any significant degree a decay of anomalous particles nor the emission of energetic fragments into wide laboratory angles with $\theta > 20°$. This result is in agreement with a similar experiment using 36 GeV ^{40}Ar instead of 25 GeV ^{12}C [2]. These two experiments are considered as being "normalizing" experiments.

B. Further experiments using two Cu disks

Here we report on a series of exposures, carried out with a wide variety of projectiles of two Cu disks in contact using the target configuration shown in Fig. 1(a).

The results for $R_0(^{24}\text{Na})$ are given in Fig. 3. In Fig. 3(a) we observe a strong linear increase of R_0 in the range $2 < E_T < 80$ GeV. Additionally, we also show in Fig. 3(b) some recent results obtained from the ^{32}S beam at the Super Proton Synchrotron (SPS) at CERN, Geneva, which extend our investigation to 6.4 TeV, the highest energy obtained in any laboratory. However, here a word of caution is required. The experiments at the SPS were carried out in a parasitic manner close to the beam dump and some 50 cm downstream of a 1 cm thick U target. Therefore, the Cu disks were irradiated with the primary heavy ions plus a considerable amount of secondary particles. Nevertheless, it may be that a saturation value of R_0 is reached for $E_T > 1$ TeV (E_T is the total kinetic energy).

When one moves the two Cu disks apart, the detector may no longer sample all fast secondary particles generated in the target. However, we know experimentally that nearly all relativistic PF (nucleons as well as heavier ones) are emitted into a narrow forward cone and the higher the energy and the energy per nucleon of the incoming ions is, the more we expect a forward-focused distribution [2]. Thus we expect in the detector Cu-4, as shown in Fig. 1(b) nearly all the activity for ^{24}Na which we observe at $d = 0$ cm in Cu-2. As Fig. 4 shows this expectation is satisfied up to about $E_T \approx 30$ GeV. However, for higher energies, we are losing increasing amounts of ^{24}Na at distances of 10–20 cm. The detector disks cover angles $\theta \leq 20°$: For ^{40}Ar we are losing (16±2)% at 72 GeV and only (3±2)% at 36 GeV [2]. A similar behavior is found for ^{12}C: We are losing (5±1)% at 44 GeV and (2±2)% at 25 GeV. The exact distances between the front and end disks are given in the caption of Fig. 4. At present, we can only repeat the two different explanations for this puzzle: It could be caused either by the decay of anomalously excited fragments to their ground state over a flight path of 10–38 cm and/or by the wide-angle emission of "energetic" particles, having the ability to produce appreciable amounts of ^{24}Na in copper, even if they are emitted into large laboratory angles $\theta \geq 20°$. We describe in Sec. III some experiments attempting to elucidate this problem.

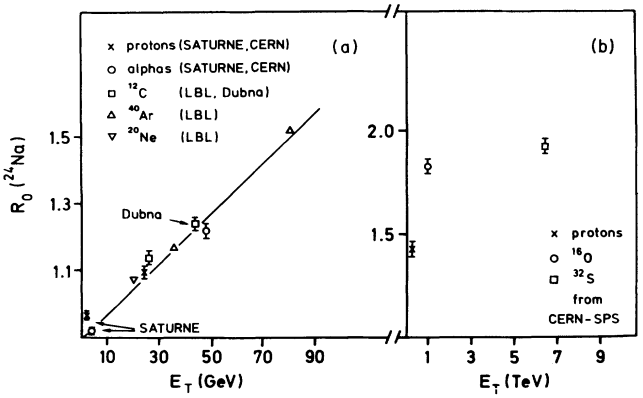

FIG. 3. The ratio $R_0(^{24}\text{Na})$ of the detector yield to the target yield with the disks in contact ($d = 0$) as a function of the total kinetic energy E_T of the incoming heavy ion. (a) For $1 < E_T < 100$ GeV. (b) For $E_T > 300$ GeV. A preliminary account has been published [4,8,15].

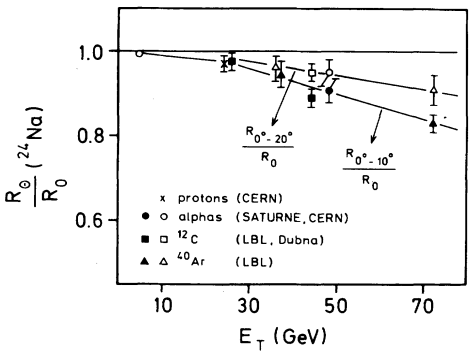

FIG. 4. The ratio $R_\theta(^{24}\text{Na})$ of separated Cu disks within certain angular ranges, e.g., $0° < \theta < 10°$ or $0° < \theta < 20°$ [4], as compared with $R_0(^{24}\text{Na})$, as a function of the energy of the incoming heavy ion. R_θ gives the activity ratios mostly at 20 cm distance. R_θ for 25 GeV ^{12}C and 24 GeV p is given for $d = 10$ cm, R_θ for 44 GeV ^{12}C is given for $d = 38$ cm. Solid symbols indicate $R_{0°-10°}$, open symbols $R_{0°-20°}$.

C. Experiments with a very thick stack of up to 16 Cu disks

In Fig. 1(c), we show a very thick stack of 16 Cu disks as a kind of calorimeter. In this paper, we describe some experiments with this setup and give some experimental results. The results are needed for empirical corrections, as described in the next section. We refrain in this article from a detailed analysis of this experiment. The stack, as shown in Fig. 1 (c), has been irradiated twice with 44 GeV ^{12}C. The results for ^{24}Na production in this very thick Cu stack are shown in Fig. 5, together with the re-

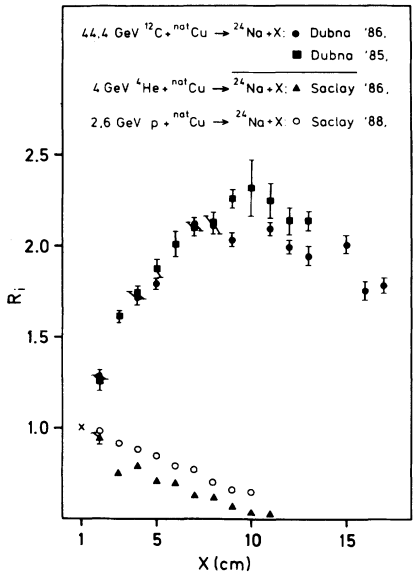

FIG. 5. The ratio R_i for ^{24}Na observed in downstream Cu disks to that in the first disk in a very compact stack of Cu disks as shown in Fig. 1(c) for four irradiations. The index (i) in R_i is given as (x/cm) on the abscissa. The cross at ($R_i = 1$; x/cm = 1) is the normalization point for all distributions.

sults of similar irradiations with 4 GeV ^{4}He and 2.6 GeV p. These results are taken from [5,13], they are shown for illustration purposes and shall be compared with results, shown later in Sec. V.

III. EXPERIMENTS WITH 44 GeV ^{12}C, USING THE 2π RING TARGET

The results of detailed experiments with copper targets irradiated with 72 GeV ^{40}Ar have been published [1–11]. This reaction channel will be studied further [50]. Consequently, it seemed interesting to supplement such work with similar investigations using the 44 GeV ^{12}C beam from the SYNCHROPHASOTRON, i.e., at lower total energy but at higher energy per nucleon. This should tell us whether unconventional effects are a general feature in high-energy heavy-ion interactions at $E_T > 40$ GeV, or whether they are specific to ^{40}Ar ions. Crucial is the question of the production of ^{24}Na from energetic secondary fragments in copper at wide angles, say, $\theta > 10°$. For this reason, we irradiated, with relativistic heavy ions, a ring-target arrangement covering to a first approximation a solid angle 2π. It will be referred to hereafter as the "2π ring target" (Fig. 6). It covers ideally a 2π solid angle for a pointlike beam and consists of two 1 cm thick Cu disks ($k=1$, front disk; $k=9$, back disk, covering $0° \le \theta \le 6°$, separated by a distance $d=38$ cm) and of seven Cu rings of different shapes in between, cut out of 1 cm thick Cu cylinders with an outer diameter of 8 cm and an inner opening of 4 cm. For an idealized pointlike beam, the seven Cu rings cover the following angular ranges: ($k=2$), 90°–70°; ($k=3$), 70°–52°; ($k=4$), 52°–43°; ($k=5$), 43°–31°; ($k=6$), 31°–19°; ($k=7$), 19°–10°; and ($k=8$), 10°–6°. This type of target was irradiated three times with 44 GeV ^{12}C: (1) at first for a period of 19 h with a total of 2.5×10^{12} ions, (2) second for a period of 17 h with a total of 1.7×10^{12} ions, and (3) at last for a period of 12 h with a total of 9×10^{11} ions. During the last irradiation, the inner front disk ($r<2$ cm) had a thickness of only 0.5 cm, i.e., one-half of that used in the first two experiments. The beam was well focused, and its beam focus was determined in experiment (1) via the ^{22}Na activity induced by the beam in the front disk ($k=1$). In experiment (2), using a ring-segmented front target, we determined the beam focus via ^{24}Na activity. Its beam spot density could be approximated by a Gaussian with a variance $\sigma=5.5$ mm during experiment (2). Details are given in the Appendix. The gamma activity in Cu was measured in the standard way. It should be pointed out, however, that the total activity in the Cu rings was not very large; this, in turn, lead to relatively larger statistical errors than in the R_0 measurements. Figure 7 shows a typical gamma spectrum in one of those rings. The experimental results for $R_\theta(^{24}\text{Na})$ in the three exposures with 44 GeV ^{12}C are given in Table I. In Table III, we give the results for a control experiment. We used a slightly modified target system, with a smaller number of Cu rings, described in the caption to Table III. It was irradiated using an independent experiment with about the same total ion flux as the first experiment. The agreement of the $R_\theta(^{24}\text{Na})$ values within Tables I and III shows that the production of ^{24}Na within one specific ring is not influenced significantly by the rings close by. As one can see from Fig. 6, primary particles from the beam halo entering the outer area of the 2π ring target ($2<r<4$ cm) propagate through a thick Cu target, such as shown in Fig. 1(c). In order to know the true wide-angle emission of energetic particles emitted from the center of the first Cu disk in Fig. 6 ($r<2$ cm), one has to correct for this beam halo thick-target effect. For this, we use the results from Fig. 5 for 44 GeV ^{12}C. We correct the experimental $R_\theta(^{24}\text{Na})$ in Table I for beam halo effects as follows: (1) We assume that we observe in the ring ($k=2$; 90°–70°) only the beam halo. (2) The upper limit for the beam halo correction in every ring is proportional to its weight (in g Cu) and proportional to the R_i value of Fig. 5. As we do not have a perfect "very compact stack" of copper, such as shown in Fig. 1(c), some energetic secondary fragments leave the copper material if they are emitted into large laboratory angles They do not contribute to the beam halo activity. Thus, a 20% reduction of the upper limit beam halo correction is considered as the lower limit beam halo correction, as approximately 20% of all energetic secondaries are emitted with $\theta > 6°$ (Tables I and II) for 44 GeV ^{12}C. For the 4 GeV ^{4}He irradiation, only an upper limit beam halo correction has been considered. (3) The correction for beam halo in Table II is taken as the mean value between the upper and lower limit beam correction, with an un-

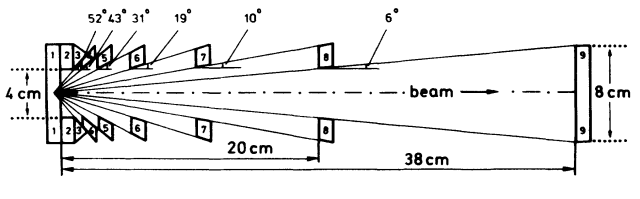

FIG. 6. The 2π ring target which was exposed to 44 GeV ^{12}C at the Dubna SYNCHROPHASOTRON. The Cu disks (1 and 9) have a diameter of 8 cm, and they are 1 cm thick. The Cu rings (2 to 8) have a shape as indicated, and their thickness is 1 cm. Details are described in the text and given in [11–15].

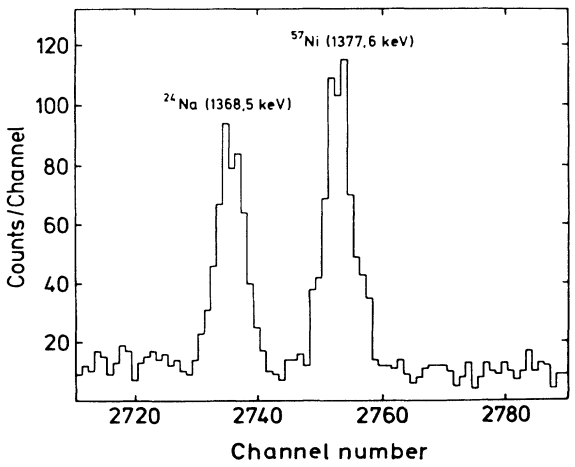

FIG. 7. A typical γ spectrum in one copper ring, as measured with a Ge(Li) detector.

TABLE I. Directly observed values $R_\theta(^{24}\text{Na})$, using the 2π ring target for 44 GeV ^{12}C. The observed experimental results for three experiments are given. $R_\theta(^{24}\text{Na})$ is the ratio of the ^{24}Na activity within a certain angular interval θ as compared to the first copper disk, in percent (see Fig. 6).

Angular interval θ	Experiment (1)	Experiment (2)	Experiment (3)
90°–70°	1.5±0.3	0.6±0.2	1.9±0.2
70°–52°	1.2±0.3	0.4±0.2	1.2±0.1
52°–43°	1.0±0.2	0.5±0.2	1.6±0.2
43°–31°	2.7±0.3	1.3±0.2	2.5±0.3
31°–19°	5.3±0.6	4.8±0.2	4.5±0.4
19°–10°	7.4±0.6	6.8±0.2	5.9±0.5
10°–6°	7.7±0.6	7.4±0.3	7.0±0.7
6°–0°	107.0±2.0	105.0±3.0	179.0±15.0
Thickness of (1) copper disk ($r<2$ cm)	1.0 cm	1.0 cm	0.5 cm[a]

[a]In experiment (3), the distance between the front plate (0.5 cm) and the end plate (1 cm) was only 20.2 cm. For calculating the given ratios, the activity of the first copper disk was doubled.

certainty spanning the entire uncertainty range. Such an uncertainty is a rather conservative estimate, but due to the limited statistical accuracy in our experiment, we consider this to be appropriate. The final results for the angular distribution $R_\theta(^{24}\text{Na})$, as corrected for beam halo effects, are given in Table II.

A similar experiment has been carried out with 4 GeV ^{4}He (Table IV). It has been mentioned already that there is no reason to expect any SMFP effects here. The target was slightly modified: the distance between the first and last Cu disk was only 20 cm and six rings were placed in between them.

From this, we can conclude the following experimental facts.

(1) The 2π ring target shows an appreciable amount of ^{24}Na produced by secondary fragments emitted into large laboratory angles ($6°<\theta<43°$) from a 1 cm thick Cu disk irradiated with 44 GeV ^{12}C. Actually, (5±1)% of the ^{24}Na activity is observed at $\theta>19°$. This is more than the (2±2)% loss of activity observed for 25 GeV ^{12}C on copper for $\theta>20°$, as shown in Sec. II A. A similar wide-angle emission is not observed for the 4 GeV ^{4}He beam.

TABLE II. $R_\theta(^{24}\text{Na})$, as observed in the 2π ring target for 44 GeV ^{12}C and corrected for beam-halo effects (see text). Only the second experiment was considered.

Angular interval θ	$R_\theta(^{24}\text{Na})$ 44 GeV ^{12}C
90°–70°	0.0±0.3
70°–52°	0.0±0.3
52°–43°	0.1±0.2
43°–31°	0.8±0.3
31°–19°	4.1±0.3[a]
19°–10°	6.0±0.3
10°–6°	6.5±0.3
6°–0°	106.0±3.0

[a]This value has been confirmed twice experimentally with segment-1,2 targets, as shown in Figs. 13 and 15.

(2) Comparing the results of the 2π geometry using 0.5 cm thick and 1.0 cm thick copper disks as targets for 44 GeV ^{12}C, we observe (Table I) the same amount of large angle activities of ^{24}Na independent of the thickness of the Cu front disk. This shows that the effect is due to primary interactions of ^{12}C.

(3) Our experiments can answer to some extent the question of whether any secondaries exhibiting the SMFP effect can be observed within our arrangement. Such an effect would show up as a significant decrease of the ^{24}Na activity in the downstream Cu configuration, when it is removed from the upstream Cu disk. When there is no such decay of secondary fragments along the flight paths shown in Fig. 6, then all the activity in the downstream Cu disk of the contact configuration [Fig. 1(a)] should be found again in the rings and in the back disk of the 2π ring target. Any loss of activity, $\Delta R_\theta(^{24}\text{Na})$, would be observed as follows:

$$\Delta R_\theta(^{24}\text{Na}) = R_0(^{24}\text{Na}) - \sum_{\theta=0°}^{90°} R_\theta(^{24}\text{Na}) \ . \quad (4)$$

The results are given in Table V. No statistically significant deviation of $\Delta R_\theta(^{24}\text{Na})$ from zero can be observed in either experiment. However, due to the experimental uncertainties in $\Delta R_\theta(^{24}\text{Na})$, we cannot exclude a contribution of decaying anomalous secondary fragments

TABLE III. $R_\theta(^{24}\text{Na})$, as observed in a control experiment with 44 GeV ^{12}C. A modified 2π ring target consisted of the front disk, only two rings ($k=5$ and $k=7$, see Fig. 6) covering the angles $43°<\theta<31°$ and $19°<\theta<10°$, and the end disk in a distance of 20 cm, covering the angle $0°<\theta<10°$. The results have not been corrected for a finite beam size. The beam size was similar to experiment (1) as shown in Table I.

Angular interval θ	$R_\theta(^{24}\text{Na})$ 44 GeV ^{12}C
43°–31°	3.2±0.3
19°–10°	7.6±0.6
10°–0°	115.0±2.0

TABLE IV. $R_\theta(^{24}\text{Na})$, as observed in the 2π ring target for 4 GeV ^{4}He. $R_\theta(^{24}\text{Na})$ has been defined in Table I.

Angular interval θ	$R_\theta(^{24}\text{Na})$ for 4 GeV ^{4}He Experimental observation	Corrected for beam halo
90°–70°	0.2±0.1	0.0±0.2
70°–52°	0.1±0.1	0.0±0.2
52°–43°	0.2±0.1	0.0±0.2
43°–31°	0.3±0.1	0.1±0.2
31°–19°	0.5±0.1	0.3±0.2
19°–10°	0.8±0.1	0.6±0.2
10°–0°	90.0±1.0	90.0±1.0

within the experimental uncertainties of 4% in $\Delta R_\theta(^{24}\text{Na})$ for 44 GeV ^{12}C and 1.5% for 4 GeV ^{4}He.

It should be recalled that the results from this experiment, where partial cross sections are measured, are not directly comparable to those in visual (i.e., emulsion and bubble chamber) experiments, where total cross sections determined the observed mean free paths. In the next section, we address the problem: Can the abundant production of ^{24}Na at large laboratory angles $\theta > 10°$ be understood within the framework of widely accepted theoretical models?

IV. CALCULATIONS USING THEORETICAL MODELS

A. Calculation for the entire angular distribution $R_\theta(^{24}\text{Na})$ $(0° < \theta < 90°)$

Obviously a complete set of multiplicities, fragmentation parameters, angular, and energy distributions of all the secondaries is needed in order to examine whether our experiments observe anything beyond conventional physics. The choice of the proper theoretical models used for the interpretation of experimental results is always a problem since no theoretical model known to the authors is suitable for the description of all the aspects of relativistic heavy-ion interactions. However, it is well known that the Dubna cascade model (DCM) is a very advanced theoretical concept [51,52], with quite a number of successful applications [53]. This model is based on the historic two-step Serber model of complex high-energy interactions: At first, we calculate a fast intranuclear cascade as a succession of nucleonic interactions. This is followed by the slow evaporation of light particles from an excited nuclear state, which is left as a residue after the fast cascading interactions. This Serber model has been refined considerably by Gudima and Toneev [51], and brought into line with many aspects of present-day high-energy phenomena, including contributions due to coalescence and precompound phenomena. Additionally, a more phenomenological model (PM) for intranuclear interactions in high-energy reactions [54] has also been used in our calculations. This model describes the interaction of a high-energy heavy ion A_1 $(0.5 < E_T < 5$ GeV/nucleon) with a target nucleus A_2. The model can be applied to target and projectile ions within the mass range $4 < A < 240$ and is concerned with the production of relativistic secondary fragments h_i, such as pions, kaons, nucleons, and hyperons. This interaction

$$A_1 + A_2 \rightarrow \sum h_i + X \tag{5}$$

(X is the target fragment) uses conventional nuclear geometry concepts in a conventional manner. The radii of both nuclei are calculated and the impact parameter b is randomly determined for each interaction by a Monte Carlo procedure. This yields the natural mixture of central and peripheral interactions. The limits between these two types of interactions are determined through an average scattering angle, which depends on A and E_T/u. For central collisions, the nuclei are subdivided row on row into cylinders, where two-body nucleon-nucleon interactions occur. For peripheral interactions, only simple nucleon-nucleon interactions are taken into account. No hydrodynamic aspects of the interactions are considered. Assuming a uniform density distribution within the interacting nuclei, the number of nucleons is calculated in both regions considered. The Fermi momentum of the constituents can be calculated by using the following phase-space distribution:

$$\frac{dn}{dp} = \frac{3p^2}{P_{FN}^3}\ , \tag{6}$$

n being the number of nucleons within the nucleus, and the momentum p is chosen randomly $[0 < |p| < P_{FN} = 0.4(n/A)^{1/3}$ GeV/$c]$. P_{FN} is the Fermi momentum. The calculation ends, when the number of target or projectile nucleons is exhausted and a further emission of nucleons is prohibited due to energy or momentum conservation. Further details are described in the original literature [54].

In our calculations using both models, we were only concerned with the emission of relativistic secondary particles (p, n, π^+, π^-, d, t, ^{3}He, and ^{4}He), during the fast cascade step. The energies and the emission angles of these particles were recorded and used for further analysis. As an example, the energy distribution and number-of-secondary particles distributions are shown in Tables VI and VII, respectively. Essentially only neutrons and protons are energetic enough to produce ^{24}Na from Cu (> 80%), as they are also quite abundant at all angles. We did not study the role of third generation particles. These fast cascade calculations gave currents N_{ijk} per

TABLE V. On the possible decay of "anomalously" large secondary fragments. The values $R_0(^{24}\text{Na})$ and $\sum R_\theta(^{24}\text{Na})$ are the results from measurements in the compact form [Fig. 1(a)] and in the 2π ring target (Fig. 6), respecitvely, $\Delta R_0(^{24}\text{Na})$ is the difference between them. $R_\theta(^{24}\text{Na})$ has been corrected for beam-halo effects (Table II).

	44 GeV ^{12}C	4 GeV ^{4}He
$R_0(^{24}\text{Na})$	1.24±0.02	0.922±0.010
$\sum_{\theta=0°}^{90°} R_\theta(^{24}\text{Na})$	1.23±0.03	0.920±0.009
$\Delta R(^{24}\text{Na})$	0.01±0.04	0.002±0.014
d[a]	38 cm	20 cm

[a]Flight path between front disk and back disk of 2π ring target.

TABLE VI. Mean energy (GeV) of secondary particles as a function of their emission angle θ. The results are obtained with the Dubna cascade model [51,52]. The model was used in a form including coalascence and precompound phenomena [14].

	41 GeV ^{12}C+^{64}Cu (2400 events)					
	0°–10°	10°–20°	20°–30°	30°–40°	40°–50°	50°–60°
$\pi^{(\pm)}$	0.90	0.71	0.50	0.38	0.30	0.24
n	2.38	0.96	0.49	0.28	0.17	0.11
p	2.40	0.99	0.53	0.31	0.18	0.12
d	2.17	0.57	0.33	0.20	0.15	0.11
t	0.45	0.25	0.19	0.16	0.13	0.10
^{3}He	1.03	0.30	0.20	0.18	0.15	0.12
^{4}He	0.08	0.08	0.10	0.10	0.07	0.05

unit time for the light relativistic particle (i) of energy E_j within a certain laboratory angular interval (k); i.e., within the acceptance of the kth ring of the 2π ring target. Then we calculated the activity A_{ijk} of ^{24}Na according to the standard equation

$$A_{ijk}=\sigma_{ij}N_{ijk}N_{\mathrm{Cu},k} \ , \tag{7}$$

where A_{ijk} is the activity of ^{24}Na in ring (k) due to particle (i) of energy E_j, σ_{ij} the cross section Cu$\rightarrow^{24}$Na for particle (i) with an energy E_j, N_{ijk} the current for particle (i) of an energy E_j within the angular interval of the ring (k), and $N_{\mathrm{Cu},k}$ number of Cu atoms (cm^{-2}) in the ring (k). We neglect terms associated with the irradiation, as they cancel in our ratio calculations. The crucial value in Eq. (7) is the cross section σ_{ij}. The most detailed description on how this cross section influences the interpretation of this type of Cu-block experiments has been given in [2]. The energy dependence of σ_{ij} (the excitation function) is known in detail only for protons and pions. The knowledge of other cross sections σ_{ij} for the yield of ^{24}Na in copper induced by other light particles, including ^{12}C is very limited. Consequently, we acted in a twofold manner.

(1) We determined three additional experimental cross sections for the reactions Cu($p/d/^{12}$C,X)^{24}Na with the following projectile energies: 8.14 GeV p, 7.3 GeV d, and 44 GeV ^{12}C, respectively. We used conventional radiochemical techniques [48,49]. The monitor cross section was ^{27}Al($p/d/^{12}$C,X)^{24}Na, and the integral particle flux could be determined with 10% accuracy. The results are given in Table VIII.

(2) In agreement with the concepts of limiting fragmentation and factorization in high-energy nuclear interactions, we always used in our calculations $\sigma_{ij}=\sigma_p(E_j)(A_1^{2/3}+A_2^{1/3})^2$ and $\sigma_{ij}=$const for $E_T>3$ GeV [2], where A_1 stands for the projectile and A_2 for the target. The resulting excitation functions are shown in Fig. 8.

The results were obtained by the DCM in the form of tabulated N_{ijk} values (see also Table VII). The calculation proceeded from Eq. (7) as follows:

$$A_{ik}=N_{\mathrm{Cu},k}\sum_j N_{ijk}\sigma_{ij} \tag{8}$$

and

$$A_k=\sum_i A_{ik} \ . \tag{9}$$

The activity A_k in the kth ring or disk is the final value needed for calculation. In order to simplify the further calculation, we compare the activity for ^{24}Na in the kth ring to the activity in the last two Cu pieces, i.e, Cu ring ($k=8$) plus the Cu back disk ($k=9$, Fig. 6). This activity is produced in the angular interval $0°\leq\theta\leq10°$ and is normalized to 1.13, as observed experimentally (Table II).

The results of the calculations for R_θ are shown in Fig. 9 and compared with the experimental results, as given in Table II. The experimental angular distribution decreases much less steeply than the calculated one. Obvious is the agreement for $R(\theta)$ in the angular interval $19°<\theta<31°$ for two independent experimental setups: the 2π target and the segment targets (to be explained in the next section). Furthermore, there is fine agreement

TABLE VII. Number of secondary particles ($dN/d\Omega$), in relative units as a function of their emission angle θ. Obtained with the Dubna cascade model [51,52].

	41 GeV ^{12}C+^{64}Cu (2400 events)					
	0°–10°	10°–20°	20°–30°	30°–40°	40°–50°	50°–60°
π^+	987	446	246	156	104	78
π^-	1050	472	268	178	125	89
n	6835	1593	910	620	455	378
p	6606	1535	813	544	386	302
d	437	199	141	116	90	70
t	29	22	18	18	15	16
^{3}He	24	20	16	14	10	10
^{4}He	18	10	16	12	13	11

TABLE VIII. Some cross sections for the reaction ^{64}Cu($p/d/^{12}$C,X)^{24}Na, as determined in this work and recently by Cho *et al.*[a]

Projectile	Energy (GeV)	$\sigma(^{24}\text{Na})$ (mb)
p	8.15	3.4±0.5
d	7.3	5.4±0.9
^{12}C	44.0	12.3±1.8
^{12}C	0.5	1.43±0.17[a]

[a]S.Y. Cho *et al.*, Phys. Rev. C **36**, 2349 (1987).

between the two independent theoretical models. The calculations are based on the assumption of a pointlike beam for primary ions. Indeed, we were able to observe a rather narrow beam distribution with a variance of $\sigma \approx 5.5$ mm for an assumed Gaussian type of beam width. Such a beam distribution influences the calculated distributions by (10–40)%, depending on the angle θ, as shown in the Appendix and Ref. [12]. The discrepancy between experiment and theory amounts now to a factor of 2.4±0.2 for the angular interval $10° < \theta < 19°$, and to a factor of 7.6±0.6 for the angular bin $19° < \theta < 31°$. Such large discrepancies are quite remarkable. In our calculations, we ignore the influence of gamma rays due to π_0 decay on ^{24}Na production: the mean energy and abundance of π_0 is similar to π^+ and π^-. Each π_0 decays into 2 gamma rays. It is well known that the electromagnetic interaction is much weaker than the strong interaction of hadrons. Charged pions, however, contribute only a small fraction (~5%) to the observed ^{24}Na activity in Cu at all angles [12–15].

Obviously, further experimental and theoretical work is needed in order to better understand this puzzle: *the abundant production of ^{24}Na at wide angles by secondary fragments produced with heavy ions at high energies* ($E_T > 40$ GeV). But the quality of our models, in particular the PM, is quite sufficient to interpret the 2π experiment with 4 GeV ^{4}He, such as shown in Fig. 10. This is in agreement with the remarks made earlier, that for $E_T < 40$ GeV we observe no significant emission of energetic secondaries into wide angles, such as for 25 GeV ^{12}C and 36 GeV ^{40}Ar.

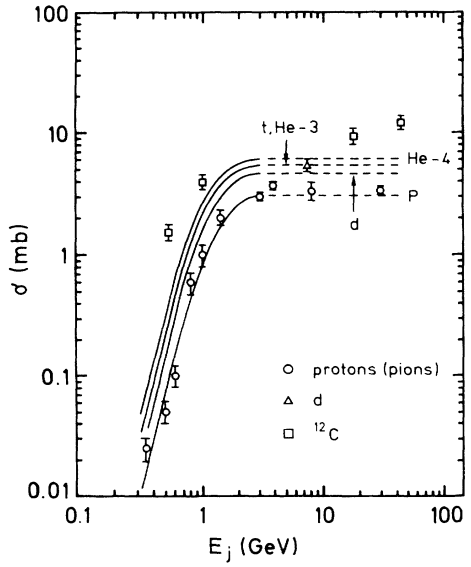

FIG. 8. Excitation function for the reaction ^{64}Cu(X,Y)^{24}Na. The experimental points are given with error bars; the four curves (for $p,d,t/^3$He, ^{4}He) are used in the calculations as described in the text.

B. Calculations within a limited angular interval ($10° < \theta < 31°$)

We now restrict our concern to a limited angular interval ($10° < \theta < 31°$) and assume that we can completely understand R_θ for $10° < \theta < 19°$. Then we calculate the following ratio:

$$R_L \equiv \frac{R(19° < \theta < 31°)}{R(10° < \theta < 19°)} . \tag{10}$$

This ratio R_L can be determined much more accurately than R_θ of the preceding section (IV A), both experimentally and theoretically: The experimentally observed and halo-corrected ratio R_L^{ex} can be determined as the ratio of ^{24}Na activities in two Cu rings ($k=6$ and $k=7$ in Fig. 6) from Table II as follows:

$$R_L^{ex} = 0.68 \pm 0.03 . \tag{11}$$

In order to calculate the ratio R_L^{th} theoretically we only need to consider the effect of high-energy pions, protons (to some extent deuterons), and neutrons, such as shown

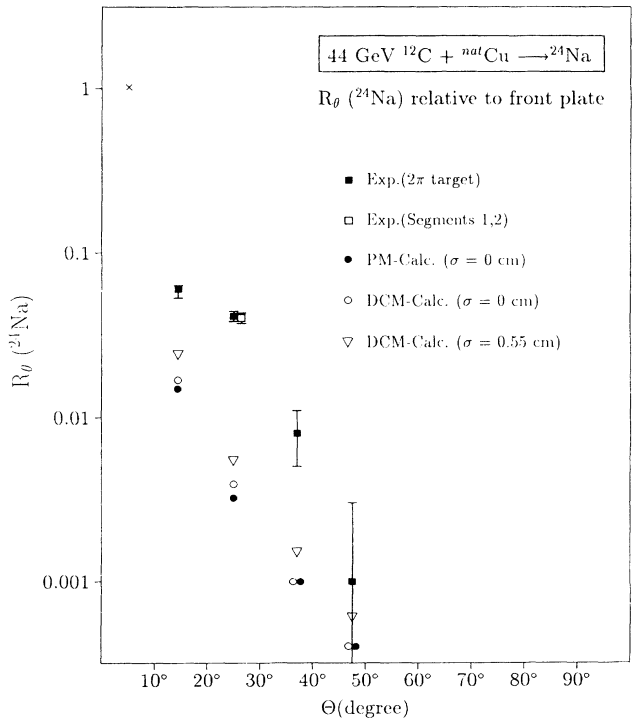

FIG. 9. Comparison between calculated and experimental distributions $R_\theta(^{24}\text{Na})$ in the reaction (44 GeV ^{12}C+^{nat}Cu) realized at the SYNCHROPHASOTRON, Dubna. All distributions are normalized to the observed ^{24}Na activity within the angular interval $0° < \theta < 10°$. PM, phenomenological model; DCM, Dubna cascade model; for details see text and Table II.

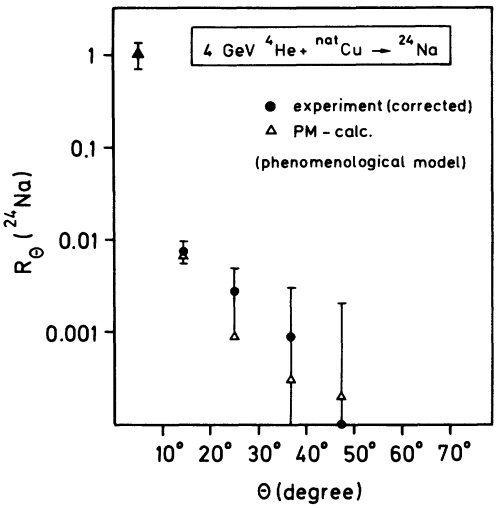

FIG. 10. Comparison between calculated and experimental distribution $R_\theta(^{24}\text{Na})$ in the reaction (4 GeV ^{4}He+^{nat}Cu) realized at the SATURNE, Saclay. All distributions are normalized to the ^{24}Na activity within the angular interval $0° < \theta < 10°$ [14].

in Tables VI and VII for the DCM. Additionally, there exists direct experimental evidence for the energy spectra in the angular interval $10° < \theta < 20°$ and $20° < \theta < 30°$, as observed for secondary pions and protons produced in the interaction of 44 GeV ^{12}C with C targets and observed by Kanarek *et al.* [55] in a bubble chamber at Dubna. In a similar work of Agakishev *et al.* [56], it was shown that the shape of energy spectra for negative pions does not change, when one uses 3.65 GeV/nucleon p,d,α, and C beams on C targets. Consequently, it is a good approximation to assume, that the energy spectrum of secondary particles does not change on the high-energy side, when one goes from C to Cu targets. The results of the comparison of energy spectra, as calculated by the DCM and observed experimentally are shown in Fig. 11, further details are summarized in Table IX. The agreement is fairly good.

Now, it is straightforward to calculate R_L^{th} for a given interval $20° < \theta < 30°$ versus $10° < \theta < 20°$, using the excitation function shown in Fig. 8:

$$R_L^{\text{th}}\left[\frac{20° < \theta < 30°}{10° < \theta < 20°}\right] = 0.21. \tag{12}$$

This ratio has to be corrected for the realistic R_L^{th}, considering the true experimentally observed angles $19° < \theta < 31°$ versus $10° < \theta < 19°$:

$$R_L^{\text{th}}\left[\frac{19° < \theta < 31°}{10° < \theta < 19°}\right]_{\sigma=0\text{ mm}} = 0.26 . \tag{13}$$

This calculated ratio holds for an idealized pencil beam ($\sigma = 0$ mm). According to a procedure shown in the Appendix (and also Ref. [12]), we now calculate for the observed beam spread $\sigma = 5.5$ mm (theory: DCM):

$$R^{\text{th}}_{L,\sigma=5.5\text{ mm}} = 0.30 . \tag{14}$$

This can be compared to the experimental value R_L^{ex}, the difference between experiment and theory is

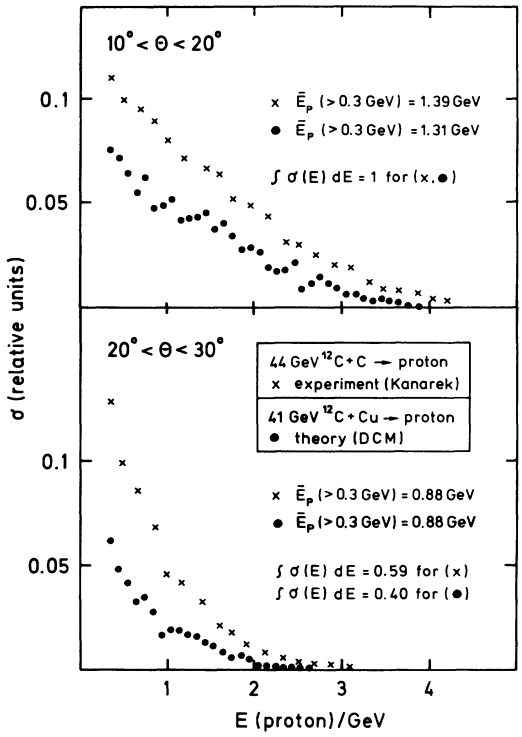

FIG. 11. Energy spectra for secondary protons emitted into certain angles θ. For the angular interval $10° < \theta < 20°$ the spectra are normalized, for the angular interval $20° < \theta < 30°$ their decrease is given. Experimental [55] and calculated [14,51,52] energy spectra are shown. (When comparing this figure with Tables VI and VII, please note, that in this figure we show only energies with $E > 0.3$ GeV and not $E > 0$ GeV, as in Tables VI and VII.)

$$\Delta(R_L) = 0.38 \pm 0.03 . \tag{15}$$

This result is shown in Fig. 12. We obviously have increasing difficulties in understanding the observed activities of ^{24}Na in Cu, when we place the Cu rings into larger laboratory angles, say, $19° < \theta < 31°$, as compared to $10° < \theta < 19°$. Due to the fact that at even larger angles ($\theta > 31°$) we observe very little ^{24}Na with rather large uncertainties, we stopped this analysis at the given angles ($\theta = 31°$).

Moreover, minimum ionizing particles (MIP, $\beta > 0.7$) are observed in nuclear emulsions under large laboratory angles. They can be either protons ($E > 370$ MeV) or points ($E > 56$ MeV) [2]. In Ref. [12], Table 3.5, the total

TABLE IX. Comparison of mean kinetic energies $\bar{E}$ for protons and pions, of energies above the thresholds ($E_p > 300$ MeV and $E_\pi > 50$ MeV). The calculation is based on the DCM [51,52] for the reaction 41 GeV ^{12}C+Cu, the experiment on results of Kanarek *et al.* [55] for the reaction 44 GeV ^{12}C+C.

	$10° < \theta < 20°$		$20° < \theta < 30°$	
	$\bar{E}_p$ (GeV)	$\bar{E}_\pi$ (GeV)	$\bar{E}_p$ (GeV)	$\bar{E}_\pi$ (GeV)
Calc.	1.39	0.66	0.88	0.53
Exp.	1.31	0.71	0.88	0.62

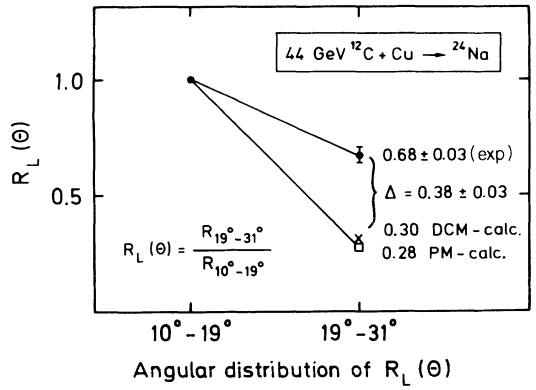

FIG. 12. Comparison between the theoretical models (DCM and PM) and the experimental angular distribution R_L in the reaction (44 GeV $^{12}C+^{nat}Cu$). The ratio R_L is normalized to the ^{24}Na activity within the angular interval $10°<\theta<19°$ and compared to $19°<\theta<31°$. Details are given in the text.

number of MIP in the interesting angular ranges $10°<\theta<19°$ and $19°<\theta<31°$ are given. This ratio $114/149=0.77\pm0.16$ is nearly the same as the one given above, $R_L^{ex}=0.68\pm0.03$. Assuming that only MIP cause the production of ^{24}Na out of Cu, this coincidence supports the idea that the energy has to be the same in both of these angular ranges. But this contradicts all empirical results (Fig. 11, Table IX, and Fig. 8).

As a result, we state: *one observes too high a ^{24}Na activity at large laboratory angles.* We are unable to account for this discrepancy. The reason could be any of the following (among others).

(1) The phenomenological model (PM) and the Dubna cascade model (DCM) take too low transverse momenta into account, but only when compared to our 44 GeV experiment. (But one should remember the agreement between the experimental and calculated energy spectra for secondary hadrons produced with 44 GeV ^{12}C as shown in Fig. 11 and Table IX.)

(2) We assumed a predominant emission of relativistic $Z=1$ hadrons (also neutrons) into wide angles. This is given by the cascading models used, and it is observed experimentally in nuclear emulsions [2,16].

(3) The emission of energetic heavy fragments ($A>4$) into large laboratory angles has been completely neglected. That this procedure is justified, is shown by the observation in CR-39 solid-state nuclear track detectors. There it was observed [8,9,57], that after the bombardment of a 1 cm thick Cu target with 44 GeV ^{12}C only a tiny fraction of such energetic fragments ($Z=6$) occurred ($\leq 10^{-4}$ as compared to primary ions). This is obviously too small a fraction to cause the effect reported on in this paper.

(4) We did not consider the anomalous hypothesis, such as formulated in Ref. [16]: here we conjectured that light hadrons (protons, neutrons, and, less likely, also pions) *may* have a considerable enhanced cross section, either total and/or partial, at the moment of their creation as secondary particles in high-energy heavy ion reactions above a certain threshold, which may be $E_T \geq 40$ GeV (see Fig. 4).

V. FURTHER CONTROL EXPERIMENTS

The enhanced production of ^{24}Na by wide angle secondaries produced in copper by 44 GeV ^{12}C has been the essential observation reported in this paper. It is desirable to have further experimental confirmations for this experimental fact. Consequently, we carried out the following control experiments.

(1) We exposed the target system segment-1 [shown schematically in Figs. 13(a) and 13(b)] over a period of 23 h to 2.5×10^{12} ions (44 GeV ^{12}C). This new setup consisted of a small Cu target T (2 cm diameter, 1 cm thick) and Cu segments, exposed to secondary fragments emitted from the center of the Cu target into polar angles $20°<\theta<30°$. These three Cu segments (A,B,C) always covered an azimuthal angle ($\varphi=38°$), so as not to interfere with each other. They were placed at increasing distances from the target T. Each segment consisted of three 1 cm thick subsegments (A_{1-3},B_{1-3},C_{1-3}). We determined in the usual way the ^{24}Na activity in all the copper pieces and carried out the proper geometrical corrections as described in detail in Refs. [8,13]. Then we normalized the activity from $\varphi=38°$ to the full azimuth of 360°. The results are given in Fig. 13(c). We observe ^{24}Na activity $R_\theta(^{24}Na)$ in all segments and subsegments

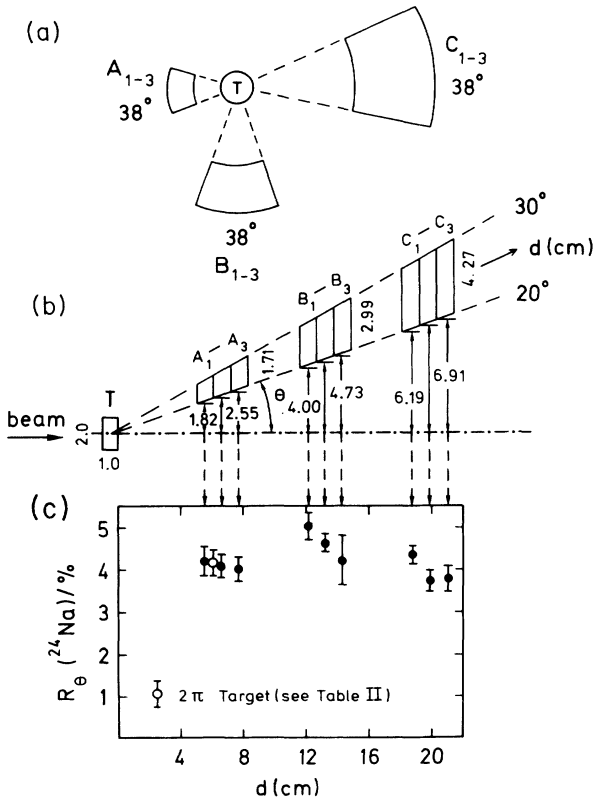

FIG. 13. The target setup segment-1 consists of Cu target T and Cu segments, A_1 up to C_3: (a) shown from head-on view and (b) shown in a simplified cutview (c) the results for ^{24}Na in Cu after an irradiation with 44 GeV ^{12}C at Dubna. $R_\theta(^{24}Na)$ is the ratio of activity in a certain segment, say, A_1 up to C_3, normalized to 2π in azimuth to that in the target T. Further details are given in the text.

to an extent of (4.0±0.5)%. This is in agreement with the $R_\theta(^{24}\text{Na})$ measurement of (4.1±0.3)% as found in the 2π ring target for the angular range $19° < \theta < 31°$ (ring $k = 6$, as shown in Fig. 6). From Fig. 13(c), one can conclude that (i) the amount of ^{24}Na found within the angular range $20° < \theta < 30°$ does not depend on the details of the two quite different constructions of Cu-target systems, shown in Figs. 13(a) and 13(b), Fig. 6, and Tables I and II; (ii) comparing the ^{24}Na activity in subsegments A_1, B_1, and C_1, we always observe the same activity, showing no dependence on the distances d, from 7 up to 20 cm, from the Cu-target T; (iii) within the limits of experimental uncertainties, the ^{24}Na activities agree within all subsegments A_{1-3}, B_{1-3}, and C_{1-3}. A similar behavior has already been shown for 2.6-GeV protons, as shown in Fig. 5. This result will be addressed in more quantitative terms in a future publication [58].

(2) We can exclude the production of ^{24}Na in segments A_1, A_2, and A_3 as being due only to an extended beam halo as follows: As shown in Fig. 14(a) we exposed a CR-39 SSNTD (solid-state nuclear track detector) in front of the Cu disk to 7×10^7 ions (44 GeV ^{12}C). The decrease of the track intensity perpendicular to the beam direction and in front of subsegment A_1 is shown in Fig. 14(b). We estimate that <2% of the primary ^{12}C beam has hit this subsegment A_1, as compared to 4% of the observed ^{24}Na activity. This shows additionally that the ^{24}Na activity in this segment is produced by energetic secondary fragments emitted from the target T into large angular ranges $20° < \theta < 30°$. But this experiment is not yet conclusive. We compare here only the beam profile for one burst of 7×10^7 ions to the beam profile of an extended 23 h irradiation with 2.5×10^{12} ions 44 GeV ^{12}C. Consequently, we have to carry out further control experiments.

(3) We irradiate a further target system. This system is called segment-2 and is shown in Fig 15. It is similar to the one shown in Fig. 13: again one has a target T (2 cm diameter, 1 cm thick) and a series of segments A, B, C, D;

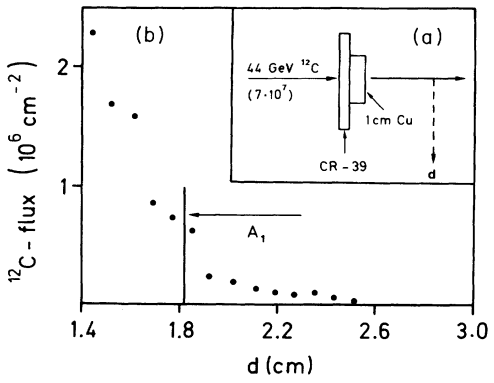

FIG. 14. (a) The experimental setup to measure the beam profile with one CR-39 plastic solid-state track detector, irradiated with one burst of a 44 GeV ^{12}C beam of the SYNCHROPHASOTRON at Dubna. (b) The decreases of the track intensity in CR-39 (identical with the decrease of the beam intensity) outside the "beam halo," as measured from the center of the target along the vector given by the segments A_1, A_2, and A_3, shown in Fig. 13.

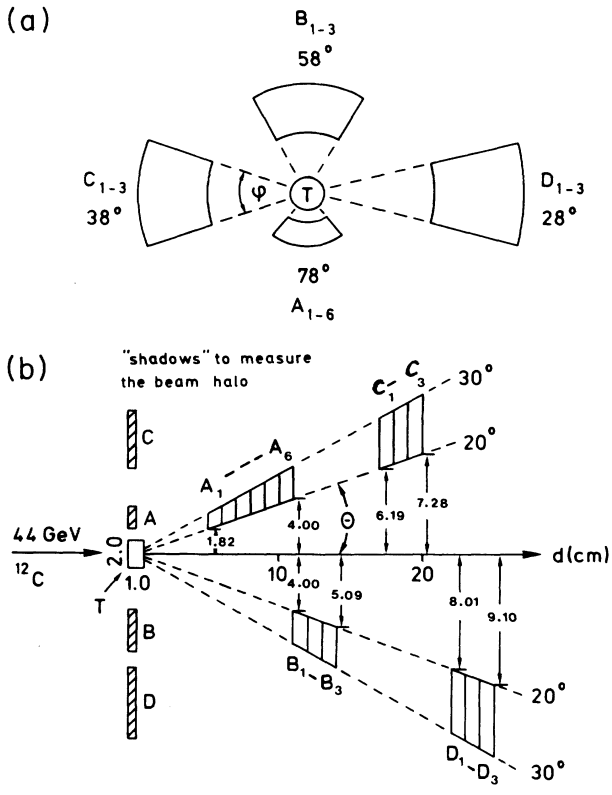

FIG. 15. The target setup segment-2 consists of a target T and Cu segments A_1 through D_3: (a) head-on view and (b) shown in a simplified cutview. Some results from this experiment are shown in the text. They concern the effect of the beam halo, as measured with the shadow to the segments A_1, B_1, C_1, and D_1. Other results will be published later [58].

the segments cover here an azimuthal angle between 28° and 78° and again a polar angle $20° < \theta < 30°$. However, we have also installed shadow copper targets; their thickness is only 0.5 cm, but their area is just the projection of the first subsegment A_1, B_1, C_1, and D_1 into the plane normal to the beam. These shadow targets determine completely the beam halo as seen by their first subsegments A_1, B_1, C_1, and D_1, respectively. In the context of this work, only one result of a 44 GeV ^{12}C irradiation with 3.5×10^{12} ions is important. We measured the ^{24}Na activity in the shadow B and in the secondary target B_1 and observed the following ratios:

$$P_s = \frac{B}{B_1} = 0.09\pm0.02\ , \quad R_s = \frac{B_1}{T} = (4.4\pm0.4)\% \ . \qquad (16)$$

The ratio P_s (0.5 cm shadow B, as compared to 1 cm thick secondary copper B_1) is significantly smaller than unity, showing conclusively, that the ^{24}Na activity found in B_1 cannot be produced by the beam halo only, but it *must* be produced predominantly by secondary fragments emitted from the target T. The ratio R_s confirms the results, obtained with the 2π and segment-1 target, already discussed. A more complete account of this experiment will be published later [58].

VI. CONCLUSION

A variety of experimental results using several Cu-target arrangements were shown and described. We find an unexpectedly large production of ^{24}Na in "secondary" copper detectors. These "secondary" copper detectors are typically 1 cm thick and are exposed to secondary particles, emitted from the interaction of 44 GeV ^{12}C within a 1 cm thick copper target. "Secondary" copper is exposed to large laboratory angles ($6° < \theta < 43°$). We reported for two theoretical models a discrepancy of a factor 7.6 ± 0.6 between experiment and theory for the production of ^{24}Na from Cu at large laboratory angles ($19° < \theta < 31°$).

We found no large production of ^{24}Na at wide angles in the interaction of 25 GeV ^{12}C with Cu. This situation resembles the results from similar experiments at 36 GeV ^{40}Ar: we observe practically no significant wide-angle production of ^{24}Na [2].

The present situation is unclear, since some aspects of our work constantly defy any attempt to be interpreted on the basis of widely accepted theoretical models. These discrepancies may reflect imperfections of the models used to describe the overall reaction mechanism in copper for primaries and secondaries alike, or they may prove that the experimental information needed to provide reliable calculations of our complex effects are simply incomplete. Consequently, we are continuing our efforts to improve the models used. We also continue our experiments.

ACKNOWLEDGMENTS

We want to thank Academic A. M. Baldin, Professor I. N. Semenyskin (Dubna), and Professor H. Baumbach (Leipzig) for their constant interest and continued support of this work. We also thank Dr. J. A. Panebratzev, Dr. A. N. Khrenov, Dr. V. A. Perevozchikov, and the SYNCHROPHASOTRON accelerator staff for technical support during the excellent irradiations in Dubna; Dr. M. Roy-Stephan, and Dr. J. Arvieux of the Laboratoire National SATURNE, Gif-sur-Yvette, for arranging very efficiently the 4 GeV He and 2.6 GeV p irradiations; Professor J. Kluberg of CERN, Geneva, for his help during the SPS irradiations; and Dr. K. Haenssgen, Leipzig, for his help during calculations. This work was supported by many institutions, among them the BMFT Bonn.

APPENDIX: ESTIMATION OF A CORRECTION FOR CALCULATED ANGULAR DISTRIBUTIONS TAKING INTO ACCOUNT THE EXTENDED BEAM SIZE OF THE 44 GeV ^{12}C BEAM

The calculations presented in this paper are based on an assumption of a pointlike beam hitting the front disk of the 2π ring-target system right in the center, as shown in Fig. 6. It is well known that the 44 GeV ^{12}C beam of the SYNCHROPHASOTRON, JINR, Dubna, is very well focused and unusually stable, even for extended irradiation periods of several days.

Nevertheless, we had to consider the small effects of an extended beam size. In the first experiment we studied for this the activity distribution of a long-lived deep-spallation product (^{22}Na, $T_{1/2} = 2.6$ yr) in Cu. We determined the ^{22}Na activity in the Cu-front disk ($k = 1$ in Fig. 6) with the help of a Ge(Li)-gamma detector. At first we measured the full disk (8 cm inner diameter), then we reduced mechanically the diameter of the disk to smaller sizes and measured again, until a central disk with 1 cm diameter remained. As one can see in Table X, practically all the ^{22}Na activity is concentrated in the central 2 cm inner diameter disk. Such a distribution can be approximated with a Gaussian shape, having $\sigma = 5.5$ mm. In the second experiment using 44 GeV ^{12}C onto a 2π ring target we measured the ^{24}Na activity in a ring-segmented front target. In this way, the beam profile, and in particular the tail of the beam, could be measured considerably more accurately. The results are given in Table XI. Again, the beam profile could be approximated with a Gaussian $\sigma = 5.5$ mm. For this very well focused beam we consider the correction factors.

We calculate the correction for the geometrical acceptance of the 2π target for an extended beam size. The angular acceptance for an ideal beam ($\sigma = 0$ mm) has already been given in Fig. 6. The model for this calculation together with the parameter used are shown in Fig. 16: $\mathbf{R}_1$ the inner radius of the copper ring (≥ 2 cm), $\mathbf{R}_2$ the outer radius of the copper ring (≤ 4 cm), $\mathbf{R}$ the vector from the center of the front disk C to the point of interaction L within the front disk ($R < 4$ cm) (the points C and L are assumed to be in the median plane of the front disk), $\mathbf{R}_0$ the vector in the Cu ring, starting at L' and directed to the point of secondary interaction I, $\mathbf{R}_p$ the vector in the Cu ring, starting from C' and ending at I ($\mathbf{R}_p$ and $\mathbf{R}_0$ are coplanar), $\mathbf{R}_i$ the vector connecting the points L and I, $\mathbf{Z}$ the vector between L and L' (this vec-

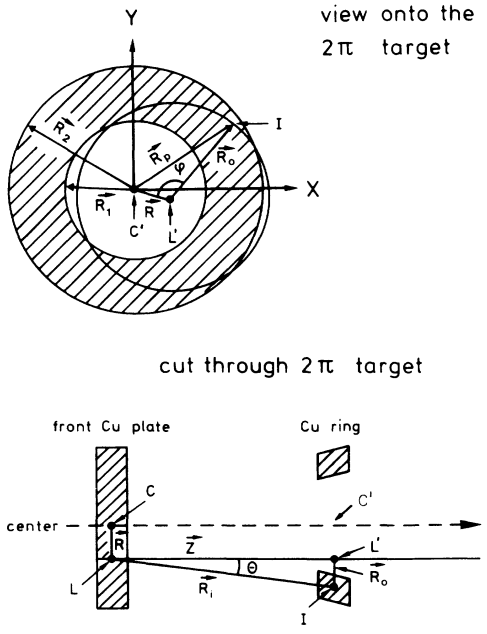

FIG. 16. Schematic drawing in order to define the parameters needed for the calculation of the effects of an extended beam size.

TABLE X. Measurement of the beam profile in the Cu front disk via ^{22}Na[a].

Diameter ϕ of Cu disk (cm)	Normalized activity of ^{22}Na ($t=0$)
8.0	6844±113
4.0	6513±124
3.5	6920±117
3.0	6971±109
2.0	6534±150
1.0	4283±104

[a]During experiment (1) with the 2π ring target exposed to 44 GeV ^{12}C ions the beam profile was measured via the induced ^{22}Na ($T_{1/2}=2.6$ yr) activity in the Cu front disk. The diameter of the disk is reduced mechanically step by step. Typically we measured at least 240 h. During this time we collected for 8 cm diameter about 5000 counts in the γ peak (1274.5 keV). Nearly all values were measured in duplicate. The beam distribution could be approximated with a Gaussian having $\sigma=5.5$ mm.

TABLE XI. Measurement of the beam profile in the Cu front disk via ^{24}Na[a].

Inner and outer diameter of Cu ring segments (cm)	Normalzied activity of ^{24}Na ($t=0$)
0–1	1386±8
1–2	979±22
2–3	134±6
3–4	15±1
4–5	4±1
5–6	3±1
6–7	3±1
7–8	3±1
0–4	2514±30
4–8	12±4[b]

[a]During experiment (2) with the 2π ring target exposed to 44 GeV ^{12}C ions the beam profile was measured via the induced ^{24}Na ($T_{1/2}=15$ h) activity in the Cu front disk. Here, this front disk was composed of ring segments as indicated in the table. The beam distribution could be approximated with a Gaussian having $\sigma=5.5$ mm.

[b]This value was obtained by comparing the ^{22}Na activity within the 0–4 cm ring segments with the 4–8 cm ring segments.

tor is parallel to the center axis), φ the angle between the two vectors $\mathbf{R}$ and $\mathbf{R}_0$ (for this operation, the vector $\mathbf{R}_0$ has been moved parallel from L' to L, i.e., from the "Cu-ring" plane to the median plane in the front disk), and θ the angle between the vectors $\mathbf{Z}$ and $\mathbf{R}_i$.

The vector $\mathbf{R}$ is Gaussian distributed around the center axis with a given variance σ. The point L with its Cartesian coordinates (X_L, Y_L) is determined randomly by two independently chosen values for the Gaussian distribution along the X and Y axis, respectively. From this we choose at random an angle φ, as defined in Fig. 16 (top), with $0<\varphi<2\pi$. Then we select an angle θ, defined in Fig. 16 (bottom), starting with $\theta=0°$ and increasing θ in steps of 1° until $\theta=75°$. After having chosen the angles φ and θ, starting from the point L, we have defined in a unique manner the vector $\mathbf{R}_i$. Now we look, whether any copper ring (i) has been hit by the vector $\mathbf{R}_i$. In the actual calculations, each Cu ring has been divided into 10 slices, each being 1 mm thick.

The calculation shows, that for an experimentally determined variance $\sigma=5.5$ mm, one must correct the calculated angular distributions (based on $\sigma=0$ mm) by about 40% within the angular interval $10°<\theta<30°$. The corrected distribution is also shown in Fig. 9. By comparing the experimental results for the two independent geometrical configurations (2π target vs segment-1) for $20°<\theta<30°$, we find the same amount of ^{24}Na in these two configurations. In addition, the ^{24}Na activity does not change with the distance from the Cu target (Fig. 13). This confirms our claim, that the statistical uncertainties of our experimental results are larger than the systematic uncertainty in the correction for an extended beam size in the 2π-target experiment.

[1] G. Dersch *et al.*, Phys. Rev. Lett. **55**, 1176 (1985).

[2] K. Aleklett *et al.*, Phys. Rev. C **38**, 1658 (1988), and references therein; **44**, 566(E) (1991) (however, the essential conclusions remain unchanged).

[3] K. Aleklett *et al.*, Symmetries and Nuclear Structure **13** (1987); in *Proceedings of the International Symposium on Symmetries and Nuclear Structure, Dubrovnik, 1986,* edited by R. A. Meyer and W. Paar (Harwood Academic, London, 1987), p. 432.

[4] K. Aleklett *et al.*, J. Radioanalyt. and Nuclear Chemistry **122**, 355 (1988).

[5] R. Brandt *et al.*, Isotopenpraxis **25**, 434 (1989).

[6] R. Brandt *et al.*, Nuclear Tracks and Radiation Measurements **15**, 383 (1988).

[7] R. Brandt *et al.*, in Proceedings of the IX International Seminar on High Energy Physics Problems, Dubna, U.S.S.R., 1988 [JINR Report D1-2-88-652, Dubna (1988)].

[8] R. Brandt *et al.*, Nuclear Tracks and Radiation Measurements **17**, 9 (1990).

[9] B. A. Arbuzov *et al.*, Nuclear Tracks and Radiation Measurements **19**, 557 (1991).

[10] R. Beckmann, Dissertation, Fachbereich Physikalische Chemie, Philipps-University, Marburg, 1984.

[11] G. Dersch, Dissertation, Fachbereich Physikalische Chemie, Philipps-University, Marburg, 1986.

[12] G. Haase, Dissertation, Fachbereich Physikalische Chemie, Philipps-University, Marburg, 1990.

[13] M. Heck, Diplomarbeit, Fachbereich Physik, Philipps-University, Marburg, 1988; Dissertation (in preparation).

[14] F. Pille, Dissertation (A), Technische Hoschschule, Leipzig, 1990.

[15] W. Schulz, Dissertation, Fachbereich Physik, Philipps-University, Marburg, 1989.

[16] E. M. Friedlander, R. W. Gimpel, H. H. Heckmann, Y. J. Karant, B. Judeck, and E. Ganssauge, Phys. Rev. Lett. **45**, 1084 (1980); Phys. Rev. C **27**, 1489 (1983), and references therein.

[17] M. M. Aggerwall *et al.*, Phys. Lett. **112B**, 31 (1982).

[18] G. N. Agakishiev *et al.*, JINR Communication PI-81-79, Dubna (1981); PI-82-795, Dubna (1982).
[19] B. P. Bannik *et al.*, Pis'ma Zh. Eksp. Teor. Fiz. **39**, 184 (1984) [JETP Lett. **39**, 219 (1984)].
[20] W. Heinrich, H. Drechsel, W. Trakowski, J. Beer, C. Brechtmann, J. Dreute, and S. Sonntag, Phys. Rev. Lett. **52**, 2402 (1984).
[21] M. L. Ticknell, P. B. Price, and S. Perlmutter, Phys. Rev. Lett. **51**, 1948 (1983).
[22] I. A. Golutvin *et al.*, JINR Rapid Communication 5-84, 8, Dubna (1984).
[23] J. D. Stevenson, J. A. Musser, and S. W. Barwick, Phys. Rev. Lett. **52**, 515 (1984).
[24] T. J. M. Symons, M. Baumgarten, J. P. Dufour, J. Girard, D. E. Greiner, P. J. Lindstrom, D. L. Olson, and H. J. Crawford, Phys. Rev. Lett. **52**, 982 (1984).
[25] I. Veres *et al.*, JINR Rapid Communication 4-84, 10, Dubna (1984); 9-85, 43 Dubna (1985).
[26] P. B. Price, M. L. Tincknell, G. Tarle, S. P. Ahlen, K. A. Frankel, and S. Perlmutter, Phys. Rev. Lett. **50**, 566 (1983).
[27] V. V. Avdejcikov *et al.*, Jad. Fiz. (Sov. J.), **44**, 440 (1986).
[28] P. L. Jain and G. Das, Phys. Rev. Lett. **48**, 305 (1982).
[29] A. G. Karev, B. A. Morozov, Yu. P. Petukhov, A. A. Povtoreyko, and A. Yu. Sukhanov, Jad. Phys. (Sov. J.) **9**, 727 (1989).
[30] A. P. Gasparian and N. S. Grigalashvili, Z. Phys. A **320**, 459 (1985).
[31] M. Bano *et al.*, Phys. Lett. **166B**, 453 (1988); **169B**, 255 (1987).
[32] V. A. Karmanov, Usp. Fiz. Nauk **140**, 523 (1983) [Sov. Phys. Usp. **26**, 636 (1983)].
[33] W. Heinrich and H. Drechsel, Proceedings of the 7th High Energy Heavy Ion Study, GSI-85-10 Report, Damstadt, **16**, 539 (1985).
[34] B. A. Arbuzov, Jad. Fiz. (Sov. J.) **42**, 542 (1985); JINR Physics of Elementary Particles and Atomic Nuclei, M. ENERGOATOMIZDAT, **19**, 5 (1988).
[35] Z. I. Soloveva, CNII atominform, vyp. I(8) (1984).
[36] B. F. Bayman and Y. C. Tang, Phys. Rep. **147**, 155 (1987).
[37] E. Ganssauge, Ann. d. Phys., 7. Folge **44**, 202 (1987).
[38] A. Milone, Nuovo Cimento **12**, 353 (1954).
[39] A. Yagoda, Nuovo Cimento **6**, 559 (1957).
[40] S. Tokunaga, T. Ishii, and K. Nishikawa, Nuovo Cimento **5**, 517 (1957).
[41] E. M. Friedlander and M. Spirchez, Nucl. Sci. Abstr. **15**, 347 (1961).
[42] B. Judek, Can. J. Phys. **46**, 343 (1968).
[43] T. F. Cleghorn, P. S. Freier, and C. J. Waddington, Can. J. Phys. **46**, 572 (1968).
[44] E. Roessle and E. Schopper, Z. Naturforsch. **9A**, 836 (1954).
[45] T. V. Varsimashvili, Zh. Eksp. Teor. Fiz. **38**, 319 (1960) [Sov. Phys. JETP **11**, 231 (1960)].
[46] G. Alexander, R. H. W. Johnston, and C. O'Ceallaigh, Nuovo Cimento **6**, 478 (1957).
[47] We are grateful to our colleagues of Ref. [2] for allowing us to include these data here. Further experimental details are given in [11].
[48] D. J. Morrissey, D. Lee, R. J. Otto, and G. T. Seaborg, Nucl. Instrum. Methods **158**, 499 (1978).
[49] G. D. Cole and N. T. Porile, Phys. Rev. C **25**, 244 (1982).
[50] H. Barth, R. Brandt, G. Dersch, G. Feige, E. M. Friedlander, E. Ganssauge, G. Haase, S. Heise, M. Heck, D. C. Hoffman, L. Lermon, W. Loveland, N. T. Porile, and G. T. Seaborg, LBL Report, University of California, Berkeley (in preparation).
[51] K. K. Gudima and V. D. Toneev, Jad. Fiz. (Sov. J.) **27**, 669 (1978).
[52] V. D. Toneev and K. K. Gudima, Nucl. Phys. **A400**, 73 (1983).
[53] D. Armutlinsky *et al.*, Z. Phys. A **328**, 455 (1987).
[54] V. G. Grishin, K. Haenssgen, and E. N. Kladintskays, JINR Communication E1-85-73, Dubna (1985); G. N. Agakishiev *et al.*, Comput. Phys. Commun. **48**, 391 (1988).
[55] H. Kanarek *et al.*, Yad. Fiz. **48**, 1752 (1988) [Sov. J. Nucl. Phys. **48**, 1054 (1988)].
[56] G. N. Agakishiev *et al.*, JINR Communicaton PI-89-793, Dubna (1989).
[57] H. H. Cui, R. Brandt, G. Dersch, and G. Haase, Nuclear Tracks and Radiation Measurements **16**, 225 (1989).
[58] R. Brandt *et al.* (unpublished).